Thin Solid Films 519 (2011) 7403–7406

Contents lists available at ScienceDirect

Thin Solid Films

journal homepage: www.elsevier.com/locate/tsf

Photoluminescence and Raman study of $Cu_2ZnSn(Se_xS_{1-x})_4$ monograins for photovoltaic applications

M. Grossberg *, J. Krustok, J. Raudoja, K. Timmo, M. Altosaar, T. Raadik

Tallinn University of Technology, Ehitajate tee 5, 19086 Tallinn, Estonia

ARTICLE INFO

Available online 21 December 2010

Keywords:
$Cu_2ZnSnSe_4$
Cu_2ZnSnS_4
Photoluminescence
Raman spectroscopy

ABSTRACT

The quaternary semiconductors $Cu_2ZnSnSe_4$ and Cu_2ZnSnS_4 have attracted a lot of attention as possible absorber materials for solar cells due to their direct bandgap and high absorption coefficient ($>10^4$ cm^{-1}). In this study we investigate the optical properties of $Cu_2ZnSn(Se_xS_{1-x})_4$ monograin powders that were synthesized from binary compounds in the liquid phase of potassium iodide (KI) flux materials in evacuated quartz ampoules. Radiative recombination processes in $Cu_2ZnSn(Se_xS_{1-x})_4$ monograins were studied by using low-temperature photoluminescence (PL) spectroscopy. A continuous shift from 1.3 eV to 0.95 eV of the PL emission peak position with increasing Se concentration was observed indicating the narrowing of the bandgap of the solid solutions. Recombination mechanisms responsible for the PL emission are discussed. Vibrational properties of $Cu_2ZnSn(Se_xS_{1-x})_4$ monograins were studied by using micro-Raman spectroscopy. The frequencies of the optical modes in the given materials were detected and the bimodal behaviour of the A_1 Raman modes of $Cu_2ZnSnSe_4$ and Cu_2ZnSnS_4 is established.

1. Introduction

Lately, the quaternary semiconductors $Cu_2ZnSnSe_4$ (CZTSe), Cu_2ZnSnS_4 (CZTS), $Cu_2CdSnSe_4$ have attracted a lot of attention as possible absorber materials for solar cells. These materials have an optimal direct bandgap for solar energy conversion and high absorption coefficients ($>10^4$ cm^{-1}) [1]. They are believed to be suitable alternatives for $CuInSe_2$ (CIS) and $Cu(InGa)Se_2$ (CIGS) absorbers since their elemental components are abundant in the Earth's crust.

Only little information about the defect structure of $Cu_2ZnSnSe_4$ and Cu_2ZnSnS_4 can be found in the literature. Raulot et al. [2] have studied the energies of defect formation of CZTSe by *ab initio* electronic structure calculations. The lowest energy of formation was found for V_{Cu} that can be considered as dominating defect in CZTSe. We have previously published a photoluminescence (PL) analysis of CZTSe monograins [3] where PL emission at 0.946 eV was attributed to an acceptor defect with an ionization energy of $E_T = 69 \pm 4$ meV. Tanaka et al. [4] have determined donor–acceptor pair recombination with a thermal activation energy of 48 meV and a PL band gap of around 1.3 eV in S-poor CZTS single crystals grown by the iodine transport method. More recently, Hönes et al. [5] have proposed a defect related recombination model for CZTS involving shallow defect levels — two shallow acceptor states 10 ± 5 meV and 30 ± 5 meV above the valence band and a donor state 5 ± 3 meV below the conduction band.

The band gap energy of CZTS is reported to be from 1.40 to 1.45 eV [5,6] to 1.51 eV [7]. For CZTSe, quite different bandgaps have been reported. Mostly, it is proposed that the band gap energy lies between 1.4 eV and 1.56 eV [8,9]. However, it was suggested by us that the band gap energy of CZTSe is about 1.02 eV according to our PL analysis [3]. Based on *ab initio* calculations Raulot et al. [2] have found a bandgap of around 0.9 eV for CZTSe.

In this paper, we study the changes in Raman spectra of the $Cu_2ZnSn(Se_xS_{1-x})_4$ solid solutions with varying sulphur to selenium concentration ratio and changes in defect structure using photoluminescence spectroscopy.

2. Experimental details

The $Cu_2ZnSn(Se_xS_{1-x})_4$ solid solutions were synthesized from CuSe(S), ZnSe(S) and SnSe(S) precursors in molten KI. More details about the synthesis can be found in [10]. The obtained material consisted of single crystalline particles with diameters of around 100 μm with tetragonal shape and rounded grain edges. The chemical composition of the monograin powders was determined by energy dispersive X-ray spectroscopy (EDS) (see Table 1). X-ray diffraction (XRD) measurements confirmed the formation of solid solutions. The monograins had p-type conductivity.

Room temperature Raman spectra were recorded by using a Horiba's LabRam HR high resolution spectrometer equipped with a multichannel CCD detection system in backscattering configuration.

* Corresponding author. Tel.: +372 6203210; fax: +372 6203367.
E-mail address: mgross@staff.ttu.ee (M. Grossberg).

0040-6090/$ – see front matter © 2010 Elsevier B.V. All rights reserved.
doi:10.1016/j.tsf.2010.12.099

Table 1
Compositions of the studied solid solutions as determined by EDS.

x	[Cu]/([Zn] + [Sn])	[Zn]/[Sn]
1	0.88	1.03
0.75	0.93	0.99
0.55	0.97	0.98
0.26	0.95	0.98
0	0.95	0.98

In micro-Raman measurements, the incident laser light with a wavelength of 532 nm can be focused on the sample within a spot of 10 μm in diameter. For PL measurements, the samples were mounted in a closed-cycle He cryostat and cooled down to 10 K. The 441 nm He-Cd laser line was used for PL excitation.

3. Results and discussion

3.1. Raman analysis

The dependence of the Raman spectra on the composition of the $Cu_2ZnSn(Se_xS_{1-x})_4$ solid solutions with x values of 1, 0.75, 0.55, 0.26 and 0, are presented in Fig. 1. The A_1 Raman mode frequencies of CZTSe and CZTS (indicated by arrows in Fig. 1) are 196 cm^{-1} and 338.5 cm^{-1}, respectively. The A_1 modes are pure anion modes which correspond to vibrations of sulphur and selenium atoms surrounded by motionless neighboring atoms [11]. A linear shift of the A_1 Raman modes of CZTS and CZTSe towards higher wavenumbers with increasing sulphur concentration in $Cu_2ZnSn(Se_xS_{1-x})_4$ is demonstrated in Fig. 2. The other Raman peaks of CZTSe were detected at 167, 172, 230, 233, and 243 cm^{-1} and the Raman peaks of CZTS at 167, 252, 288, 347, and 366 cm^{-1} (labeled with numbers in Fig. 1). The lattice vibrational properties of these solid solutions have not been discussed so far.

All Raman spectra of the studied $Cu_2ZnSn(Se_xS_{1-x})_4$ solid solutions show peaks of some secondary (mostly binary) phases (positions of the peaks are indicated by dotted lines in Fig. 1). However, the Raman peaks corresponding to additional phases have very low intensities in comparison with the CZTSe or CZTS peak intensities. All Raman spectra were fitted using Lorentzian functions to resolve the peaks. In the Raman spectrum of CZTSe the presence of ZnSe (peak at 249 cm^{-1}) was detected and also a $SnSe_2$ phase might be present (peak at 191 cm^{-1}). The corresponding Raman frequencies of ZnSe and $SnSe_2$ reported in the literature are 252 cm^{-1} [12] and

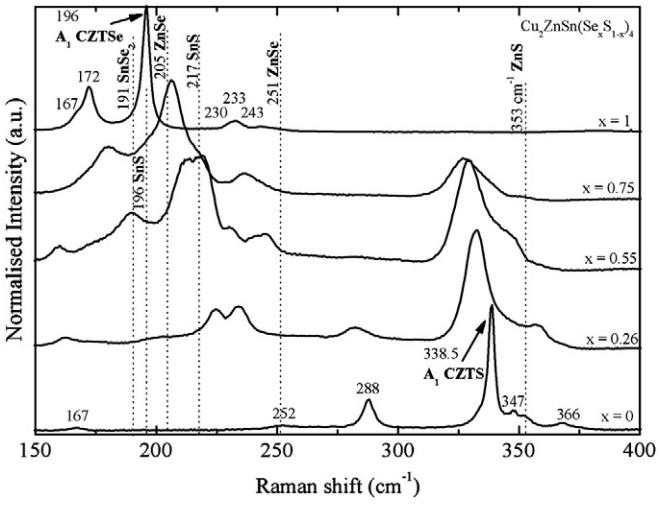

Fig. 1. Room-temperature Raman spectra of $Cu_2ZnSn(Se_xS_{1-x})_4$ solid solutions with different Se/S concentration ratio. The A_1 modes of $Cu_2ZnSnSe_4$ and Cu_2ZnSnS_4 show bimodal behaviour.

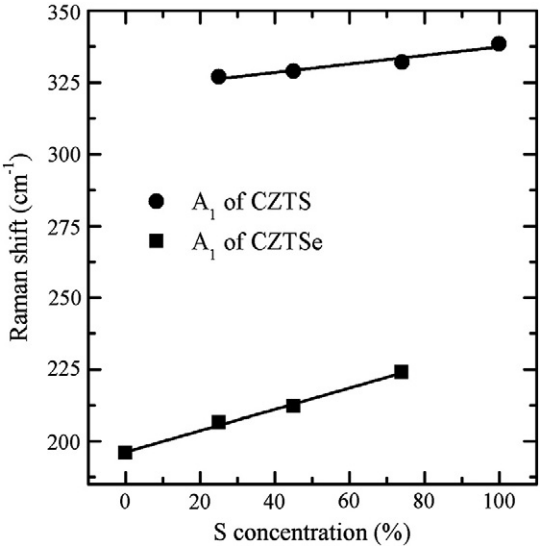

Fig. 2. CZTS and CZTSe A_1 Raman mode frequency dependencies on the sulphur concentration in $Cu_2ZnSn(Se_xS_{1-x})_4$ solid solutions. The A_1 mode of both compounds shifts approximately linearly towards higher wavenumbers with increasing sulphur concentration.

186 cm^{-1} [13], respectively. In $Cu_2ZnSn(Se_{0.75}\ S_{0.25})_4$ the presence of ZnS (peak at 353 cm^{-1}) and SnS (peaks at 196 cm^{-1} and 217 cm^{-1}) was detected. According to literature data, the corresponding Raman frequencies of ZnS and SnS are 353 cm^{-1} [14] and 192 cm^{-1} and 218 cm^{-1} [15], respectively. In the spectrum of $Cu_2ZnSn(Se_{0.55}\ S_{0.45})_4$ the presence of ZnS was detected (peak at 351 cm^{-1}) and in the spectrum of $Cu_2ZnSn(Se_{0.26}\ S_{0.74})_4$ peaks of ZnSe (peaks at 205 cm^{-1} and 251.5 cm^{-1}) and ZnS (peak at 351 cm^{-1}) were observed. In the spectrum of CZTS, a ZnS peak at 355 cm^{-1} was observed. Small deviations of peak positions of the secondary phases in the solid solutions can also be the result of a formation of solid solutions of binary compounds.

The Raman peaks of $Cu_2ZnSn(Se_xS_{1-x})_4$ solid solutions broaden with increasing sulphur content, giving the largest widths of the peaks for $Cu_2ZnSn(Se_{0.55}S_{0.45})_4$. This trend is correlated with the increasing structural disorder due to the random distribution of S and Se atoms in the lattice that leads to fluctuations in the masses and force constants in the neighborhood.

Fig. 2 presents the shift of the two A_1 modes with S concentration. As can be seen, the shift is larger for the CZTSe A_1 peak. This has also been observed in the case of $CuInS_{2x}Se_{2(1-x)}$ crystals [16]. The force constants are responsible for the trends in the frequencies of the A_1 mode. Both of the A_1 Raman modes of CZTSe and CZTS followed the two-mode behaviour throughout the entire alloy concentration range.

3.2. Photoluminescence analysis

Normalised photoluminescence spectra of the $Cu_2ZnSn(Se_xS_{1-x})_4$ solid solutions with different Se/S concentration ratios measured at T = 10 K are presented in Fig. 3. Each spectrum (except for the one corresponding to Cu_2ZnSnS_4 that is fitted with two asymmetric PL bands) consists of one asymmetric PL band. The PL bands shift towards higher energies (see Fig. 4) and become more asymmetric with increasing S concentration. Broadening of the PL bands with increasing S concentration is also observed. PL bands with such an asymmetric shape and behaviour are often observed in ternary chalcopyrites such as $CuInSe_2$ [17], $CuGaSe_2$ [18] and others that contain large concentrations of charged defects. One would expect similar results from quaternary compounds that are derived from the

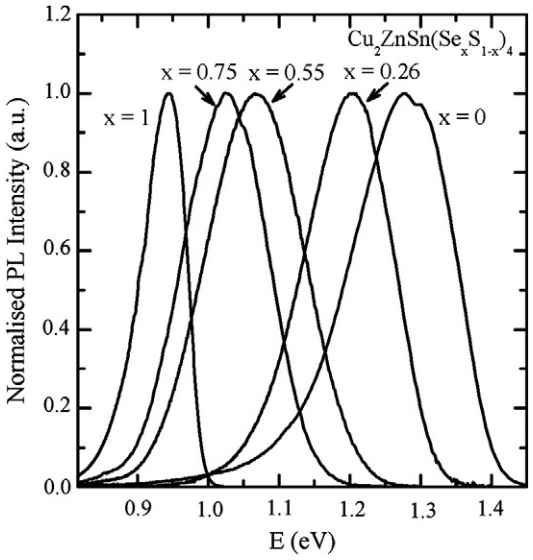

Fig. 3. Normalised low-temperature photoluminescence spectra of the $Cu_2ZnSn(Se_xS_{1-x})_4$ solid solutions with different Se/S concentration ratios. A nearly linear shift of the PL emission towards higher energies with increasing S concentration was observed up to a total value of 0.4 eV.

ternaries by substituting half of the group III element (In) by a group II element (Zn) and the other half by a group IV element (Sn).

In a semiconductor with a random distribution of high concentrations of charged donors and acceptors spatial fluctuations of the electrostatic potential are formed. These potential fluctuations will lead to a local perturbation of the band structure, thus broadening the defect level distribution and forming band tails [19]. Since the effective mass of an electron is much smaller than the effective mass of a hole in all direct-gap semiconductors, the electrons do not localize and the density of states near to the conduction band edge can be ignored. Radiative recombination in these "heavily doped" crystals is therefore often governed by the recombination of free electrons and holes localised in spatially separated potential wells originating from Coulomb potential fluctuations.

Excitation power dependent and temperature dependent PL measurements of the solid solutions performed in the present study

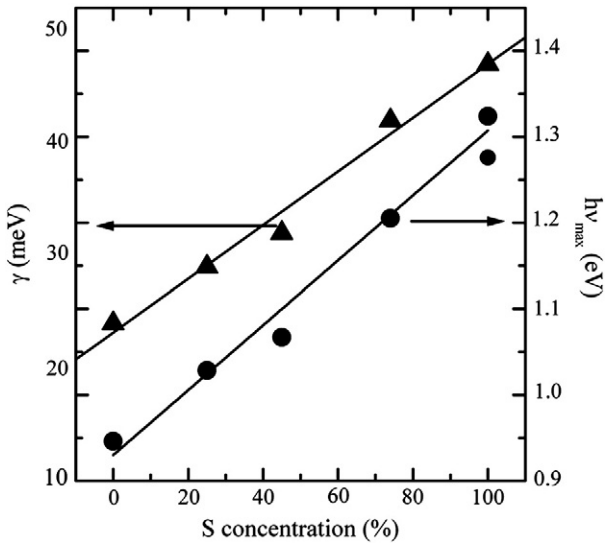

Fig. 4. Approximately linear dependence of the PL band position and the average depth of potential fluctuations γ on the S concentration in $Cu_2ZnSn(Se_xS_{1-x})_4$ solid solutions.

indicate that the PL spectra of $Cu_2ZnSn(Se_xS_{1-x})_4$ are dominated by a band-to-impurity (BI) type recombination that involves free electron and a hole in the acceptor state that is deep enough not to overlap with the valence band tail. In the excitation power dependencies a large blue-shift with a magnitude of about 15 meV per decade was detected. In addition, a non-linear dependence of the $lnI(T)$ versus $1000/T$ at higher temperatures was detected. That is common behaviour of "heavily doped" semiconductors [17,18].

In case of one of the end members (Cu_2ZnSnS_4), the origin of the lower energy PL band is not clear since no detailed analysis of this PL band could have been performed due to its low intensity.

In the case of a material that contains a large concentration of charged defects an important aspect to consider is the average depth of the potential fluctuations γ that is the mean difference of the energy of holes in the valence band fluctuation minimum and maximum. These fluctuations are expected to reduce the efficiency of the corresponding solar cells [20]. The low-energy tail of the PL bands is correlated to the average depth of the potential fluctuations γ [19] and was therefore used to estimate it.

Siebentritt et al. [21] have analyzed the shape of the band tails in the case of fluctuating potentials for thin-film materials using two different models. According to them, the low-energy tail of asymmetrical PL bands can be described by a Gaussian or an exponential spectral dependence. This is based on the more general theoretical analysis of the density of states function by Osipov and Levanyuk [19].

The low-energy side of the PL band of the end members of the $Cu_2ZnSn(Se_xS_{1-x})_4$ solid solutions analyzed in the present paper exhibit an exponential decay while the other members can be described by the Gaussian shape. This is an indication of the presence of deeper fluctuations within the samples containing both sulphur and selenium. As in [21], the average amplitude of the potential fluctuations (see Fig. 4) in the solid solutions was determined from the exponential and Gaussian spectral dependencies, respectively [19]:

$$I(E) \sim exp\left(-\frac{E}{\gamma}\right) \text{ or } I(E) \sim exp\left(-\frac{(E-E_0)^2}{2\gamma^2}\right), \quad (1)$$

where E_0 is assumed to represent an average emission energy in the case of fluctuating potentials. As can be seen from Fig. 4, γ increases with increasing S concentration in the solid solutions, being highest for CZTS. Analyzing the corresponding Raman spectra one would expect that γ is smaller in CZTS and CZTSe than in the solid solutions, because of the lower defect concentration. It has been found by Raulot et al. [2] that all selenium and sulphur compounds have a Cu vacancy formation energy close to the $CuInSe_2$, $CuGaSe_2$ and $CuInS_2$, $CuGaS_2$ values, respectively. The sulphur compounds have a V_{Cu} formation energy about 0.5 eV larger than the selenides [2]. Therefore one would expect a lower concentration of copper vacancies in CZTS compared with CZTSe resulting also in a smaller γ. One possible explanation of the obtained opposite result (Fig. 4) is the complexity of the phase diagrams of CZTSe and CZTS. The domain of a homogenous material in case of CZTS seems to be very narrow compared to CZTSe, resulting therefore in a more probable formation of other phases during the growth of the powder [22,23]. Despite the fact that γ is expected to increase due to the increasing defect concentration, we propose that in this case larger potential fluctuations are related to the presence of a defect phase or defect region that has a larger defect concentration and therefore also a higher γ value. At the same time these high γ values can be a result of compositional fluctuations, where some crystal regions have different band gap energy than others. The same behaviour was observed in $CuGa_3Se_5$ crystals [24]. The different band gap energy can be caused by different crystal structure in case of solid solutions. It was shown that, for example, that the band gap energy of kesterite-CZTS is about 0.12 eV larger than that of stannite-CZTS [25]

and both structures are possible in solid solutions. The relative concentration of the defect phase increases with increasing S concentration due to the weaker tolerance to deviations from stoichiometry in the case of CZTS. Due to the similarity of the PL properties of CZTS and the proposed defect phase one would assume that this phase has very similar properties to CZTS. Here we can see an analogy to the properties of ternary chalcopyrites where the formation of so-called ordered defect compounds have been detected [26]. However, this assumption needs further investigation.

4. Conclusions

We studied the optical properties of $Cu_2ZnSn(Se_xS_{1-x})_4$ monograin powders using PL and Raman spectroscopy. The bimodal behaviour and a shift towards higher frequencies of the A_1 Raman modes of CZTSe and CZTS with increasing S concentration were established. From PL analysis a widening of the bandgap of the solid solutions with increasing S concentration was observed. A BI recombination was detected as the main radiative recombination channel in the monograins. The average depth of the potential fluctuations present in the samples was estimated and was found to increase with increasing S concentration.

Acknowledgements

This work was supported by the Estonian Science Foundation grant G-8282 and by the target financing by HTM (Estonia) No. SF0140099s08. Support of the World Federation of Scientists National Scholarship Programme and EAS is gratefully acknowledged.

References

[1] K. Ito, T. Nakazawa, Jpn. J. Appl. Phys. 27 (1988) 2094.
[2] J.M. Raulot, C. Domain, J.F. Guillemoles, J. Phys. Chem. Solids 66 (2005) 2019.
[3] M. Grossberg, J. Krustok, K. Timmo, M. Altosaar, Thin Solid Films 517 (2009) 2489.
[4] K. Tanaka, Y. Miyamoto, H. Uchiki, K. Nakazawa, H. Araki, Phys. Stat. Sol. 203 (2006) 2891.
[5] K. Hönes, E. Zscherpel, J. Scragg, S. Siebentritt, Phys. B 404 (2009) 4949.
[6] H. Katagiri, N. Ihigaki, T. Ishida, K. Saito, Jpn. J. Appl. Phys. 40 (2001) 500.
[7] K. Ito, T. Nakazawa, Jpn. J. Appl. Phys. 27 (1988) 2094.
[8] G. Suresh Babu, Y.B. Kishore Kumar, P. Uday Bhaskar, V. Sundara Raja, Semicond. Sci. Technol. 23 (2008) 1.
[9] Rachmat Adhi Wibowo, Woo Seok Kim, Eun Soo Lee, Badrul Munir, Kyoo Ho. Kim, J. Phys. Chem. Solids 68 (2007) 1908.
[10] M. Altosaar, J. Raudoja, K. Timmo, M. Danilson, M. Grossberg, J. Krustok, E. Mellikov, Phys. Stat. Sol. 205 (2008) 167.
[11] H. Neumann, Helv. Phys. Acta 58 (1985) 337.
[12] G. Perna, M. Lastella, M. Ambrico, V. Capozzi, Appl. Phys. A 83 (2006) 127.
[13] G. Lucovsky, J.C. Mikkelsen Jr., W.Y. Liang, R.M. White, R.M. Martin, Phys. Rev. B 14 (1976) 1663.
[14] Young-Moon Yu, M.-H. Hyun, S. Nam, D. Lee, O. Byungsung, K.-S. Lee, Pyeong Yeol Yu, Yong Dae Choi, J. Appl. Phys. 91 (2002) 9429.
[15] H.R. Chandrasekhar, R.G. Humphreys, U. Zwick, M. Cardona, Phys. Rev. B 15 (1977) 2177.
[16] R. Bacewicz, W. Gebicki, J. Filipowicz, J. Phys. Condens. Matter 6 (1994) L777.
[17] J. Krustok, H. Collan, M. Yakushev, K. Hjelt, Phys. Scr. T79 (1999) 179.
[18] J. Krustok, J. Raudoja, M. Yakushev, R.D. Pilkington, H. Collan, Phys. Stat. Sol. 173 (1999) 483.
[19] A.P. Levanyuk, V.V. Osipov, Sov. Phys. Usp. 24 (1981) 187.
[20] J.H. Werner, J. Mattheis, U. Rau, Thin Solid Films 480–481 (2005) 399.
[21] S. Siebentritt, N. Papathanasiou, M.Ch. Lux-Steiner, Phys. B 376–377 (2006) 831.
[22] I.D. Olekseyuk, I.V. Dudchak, L.V. Piskach, J. Alloy. Comp. 368 (2004) 135.
[23] I.V. Dudchak, L.V. Piskach, J. Alloy. Comp. 351 (2003) 145.
[24] M. Grossberg, J. Krustok, A. Jagomägi, M. Leon, E. Arushanov, A. Nateprov, I. Bodnar, Thin Solid Films 515 (2007) 6204.
[25] S. Chen, X.G. Gong, A. Walsh, S.-H. Wei, Appl. Phys. Lett. 94 (2009) 041903.
[26] S.B. Zhang, S.H. Wei, A. Zunger, Phys. Rev. B 57 (1998) 9642.